Available online at www.sciencedirect.com
ScienceDirect
Journal of Solid State Chemistry 179 (2006) 3238–3251
JOURNAL OF SOLID STATE CHEMISTRY
www.elsevier.com/locate/jssc

The $A_{1-x}UNbO_{6-x/2}$ compounds ($x = 0$, A = Li, Na, K, Cs and $x = 0.5$, A = Rb, Cs): from layered to tunneled structure

S. Surblé, S. Obbade*, S. Saad, S. Yagoubi, C. Dion, F. Abraham

Unité de Catalyse et de Chimie du Solide, UCCS UMR CNRS 8181, USTL, ENSCL-B.P. 90108, 59652 Villeneuve d'Ascq Cedex, France

Received 23 March 2006; received in revised form 12 June 2006; accepted 18 June 2006
Available online 21 June 2006

Abstract

Attempts to prepare alkaline metal uranyl niobates of composition $A_{1-x}UNbO_{6-x/2}$ by high-temperature solid-state reactions of A_2CO_3, U_3O_8 and Nb_2O_5 led to pure compounds for $x = 0$ and A = Li (**1**), Na (**2**), K (**3**), Cs (**4**) and for $x = 0.5$ and A = Rb (**5**), Cs (**6**). Single crystals were grown for **1**, **3**, **4**, **5**, **6** and for the mixed $Na_{0.92}Cs_{0.08}UNbO_6$ (**7**) compound. Crystallographic data: **1**, monoclinic, $P2_1/c$, $a = 10.3091(11)$, $b = 6.4414(10)$, $c = 7.5602(5)$ Å, $\beta = 100.65(1)$, $Z = 4$, $R_1 = 0.054$ (w$R_2 = 0.107$); **3, 5** and **7** orthorhombic, *Pnma*, $Z = 8$, with $a = 10.307(2)$, $10.272(4)$ and $10.432(3)$ Å, $b = 7.588(1)$, $7.628(3)$ and $7.681(2)$ Å, $c = 13.403(2)$, $13.451(5)$ and $13.853(4)$ Å, $R_1 = 0.023$, 0.046 and 0.036 (w$R_2 = 0.058$, 0.0106 and 0.088) for **3**, **5** and **7**, respectively; **6**, orthorhombic, *Cmcm*, $Z = 8$, and $a = 13.952(3)$, $b = 10.607(2)$ Å, $c = 7.748(2)$ Å, $R_1 = 0.044$ (w$R_2 = 0.117$).

The crystal structure of **1** is characterized by $^2_\infty[UNbO_6]^-$ layers of uranophane sheet anion topology parallel to the (100) plane. These layers are formed by the association by edge-sharing of $^1_\infty[UO_5]^{4-}$ chains of edge-shared UO_7 pentagonal bipyramids and $^1_\infty[NbO_4]^{3-}$ chains of corner-shared NbO_5 square pyramids alternating along the [010] direction. The Li^+ ions are located between two consecutive layers and hold them together; the Li^+ ions and two layers constitute a neutral "sandwich" $\{(UNbO_6)^-$–$(Li)_2^{2+}$–$(UNbO_6)^-\}$. In this unusual structure, the neutral sandwiches are stacked one above another with no formal chemical bonds between the neutral sandwiches.

The homeotypic compounds **3**, **5**, **6**, **7** have open-framework structures built from the association by edge-sharing in two directions of parallel $^1_\infty[UO_5]^{4-}$ chains of edge-shared UO_7 pentagonal bipyramids and $^1_\infty[Nb_2O_8]^{6-}$ ribbons of two edge-shared NbO_6 octahedra further linked by corners. In **3**, **5** and **7**, the mono-dimensional large tunnels created in the [001] direction by this arrangement can be considered as the association by rectangular faces of two columns of triangular face-shared trigonal prisms of uranyl oxygens. In **3** and **7**, all the trigonal prisms are occupied by the alkaline metal, in **5**, they are half-occupied. In **6**, the polyhedral arrangement is more symmetric and the tunnels created in the [010] direction are built of face-sharing cubes of uranyl oxygens totally occupied by the Cs atoms. This last compound well illustrates the structure-directing effect of the conterion.

Keywords: Alkaline uranyl niobates; Crystal structure; Solid-state synthesis; Layered structure; Tunneled structure

1. Introduction

As a part of the ongoing research on the synthesis and the crystal structure studies of compounds obtained from the condensation of uranyl bipyramidal polyhedra (square, pentagonal or hexagonal bipyramids) and oxoanions such as silicate [1–3], phosphate [4–6], molybdate [7–16] or tungstate [17–20], recent studies in our group have focused on the uranyl–vanadate system [21–28]. Surprisingly, no recent report concern the uranyl niobates although some similarities exist between the U–V–O and U–Nb–O systems. For example, UMO_5 and UM_3O_{10} that contain U^{5+} adopt the same structures for both M = V [29–32] and Nb [33–35]. In addition, some uranium–niobium-containing oxides have structures based on very common types such as perovskite in the A cation-deficient perovskite UNb_4O_{12} [36], pyrochlore in $(U, Na)_{2-x}Nb_2O_{7-y}$ [37] or tetragonal bronze in $(Nb_{7.6}U_{2.4})(Ba_{5.2}K_{0.8})O_{30}$ [38].

*Corresponding author. Fax: +33 3 20 43 68 14.
E-mail address: said.obbade@ensc-lille.fr (S. Obbade).

0022-4596/$ - see front matter © 2006 Elsevier Inc. All rights reserved.
doi:10.1016/j.jssc.2006.06.017

Majority of the alkaline metal uranyl vanadates adopts layered structures built from the association of uranyl bipyramids and various vanadium polyhedra, tetrahedra in $(UO_2)_3(VO_4)_2 \cdot 5H_2O$ [23], the alkaline uranyl vanadate series $A_6U_5V_2O_{23}$ (A = Na, K, Rb) [22,24] and the oxychloride compounds $A_7U_8V_2O_{32}Cl$ (A = Rb, Cs) [25], square pyramids in $CsUV_3O_{11}$ [21] and in $AUVO_6$, A = Na, K, Rb, Cs, Ag [31,39–43], a family deriving from the carnotite mineral. A three-dimensional arrangement has been recently reported in the uranyl vanadates $A(UO_2)_4(VO_4)_3$ (A = Li, Na) within a novel open-framework with non-crossing channels [27].

The extended inorganic architectures formed in uranyl-containing compounds are governed in part by the geometry of the oxoanion (tetrahedron, square pyramid, octahedron, etc.) but also by the alkaline cation, which plays a key role in both connectivity and dimensionality of the obtained crystal structures. For example, $AUMO_6$ compounds have been characterized both for M = V and Nb and adopt layered structures. In $AUVO_6$, A = Na, K, Cs, Ag [31,39–43], the $^2_\infty[(UO_2)_2V_2O_8]^{2-}$ layers are built from UO_7 pentagonal bipyramids linked by $[V_2O_8]^{6-}$ units formed by two inverse VO_5 square pyramids sharing an edge. In $AUNbO_6$, A = K, Rb, the $^2_\infty[(UO_2)NbO_4]^-$ layers are built from edge sharing of two types of chains formed from edge-sharing UO_5 pentagonal bipyramids and corner-shared NbO_5 triangular bipyramids, respectively [44]. Astonishingly, $CsUNbO_6$ adopts a structure derived from the carnotite as the $AUVO_6$ compounds [45]. Surprisingly, with Tl, a tunneled structure was obtained for the compound $Tl_{0.5}UNbO_{5.75}$ [44].

The structure-directing effect of the countercation is also well illustrated by the alkaline metal uranyl tungstate, while Na, K, Rb occupy the interspace between layers formed by the linkage of uranyl and tungstate polyhedra [16–18], the smaller Li countercation leads to the formation of frameworks [19].

To explain the role of the alkaline metal, we decided a systematic reinvestigation of the A–U–Nb–O systems. The purpose of the present paper is to report synthesis of $AUNbO_6$ (A = Li, Na, K, Cs) and $A_{0.5}UNbO_{5.75}$ (A = Rb, Cs) compounds and to compare their crystal structures.

2. Experimental

2.1. Crystal and powder synthesis

For each alkaline metal, powder samples were synthesized by a solid-state reaction between mixtures of A_2CO_3 (A = Li, Na, K, Rb, Cs, Aldrich), Nb_2O_5 (Prolabo) and U_3O_8 (Prolabo) in two molar ratios: 1:1:2/3 and 1/2:1:2/3 corresponding to the hypothetic compounds $AUNbO_6$ and $A_{0.5}UNbO_{5.75}$, respectively. Mixed starting materials in the appropriate stoichiometries were heated in platinum crucibles in air successively at 800 °C for 24 h and at 1000 °C for 100 h with an intermediate grinding. The achievement of the synthesis process for each sample was controlled by X-ray powder diffraction using a Guinier-De Wolff focusing camera and Cu$K\alpha$ radiation.

For each composition, to obtain single crystals, a second batch was prepared according to the precedent process and finally melted in a platinum crucible during 48 h at 1300 °C, except for the $NaUNbO_6$ composition for which the final temperature was 1350 °C. The melted samples were finally slowly cooled at 1 °C/min to room temperature.

2.2. Powder compounds characterization

For each compound, powder X-ray diffraction data used for lattice parameters refinement were recorded on a Bruker D8 $\theta/2\theta$ diffractometer, at room temperature, using Bragg–Brentano geometry, with a back-monochromatized Cu($K\alpha$) radiation. The diffraction patterns were scanned over the range 5–100°(2θ) in steps of 0.02°(2θ) and a counting time of 20 s per step. The unit cell parameters were refined by a least-squares procedure from the indexed powder reflections.

The densities were measured with an automated Micromeritics Accupyc 1330 helium pycnometer using a 1-cm^3 cell.

To study the thermal stability of the compounds, differential thermal analyses (DTA) was performed in air with a SETARAM 92-1600 thermal analyzer in the temperature range of 20–1200 °C with heating and cooling rates of 2 °C/min, using platinum crucibles. For all compounds, no peak has been observed in this temperature range. The powder X-ray diffraction analysis of the residues after DTA measurement, confirms the only existence of the starting single phases.

2.3. Single crystal X-ray diffraction

Well-shaped crystals for $LiUNbO_6$ (**1**), $Na_{0.92}Cs_{0.08}UNbO_6$ (**7**), $KUNbO_6$ (**3**), $Rb_{0.5}UNbO_{5.75}$ (**5**), and $Cs_{0.5}UNbO_{5.75}$ (**6**) were selected for structure determinations. Each single crystal was mounted on a Bruker Platform three circles X-ray diffractometer equipped with a 1 K SMART CCD detector and operated at 50 kV and 40 mA. For each compound, preliminary unit cell parameters were determined from 30 frames with 20 s exposure times using SMART and the intensities of reflections for a sphere were measured with a graphite monochromated Mo$K\alpha$ radiation, using a combination of three sets of 600 frames, where each frame covered a range of 0.3° in ω scan. Thus, a total of 1800 frames were collected with an exposure time of 50 s per frame. The intensity reduction and correction of Lorentz, polarization and background effects, were done by the program SAINTPLUS 6.02 [46]. For each single crystal data, absorption corrections based on the precise crystal morphology and indexed crystal faces were applied using the program XPREP of the SHELXTL package [47] followed by SADABS program [48]. The crystal structures were solved by a combination of direct methods and difference Fourier syntheses, and refined by full matrix least squares against F^2, using SHELXTL package of programs [47].

3. Results

3.1. Syntheses

Pure powder samples were obtained corresponding to $AUNbO_6$ for $A = Li$ (**1**), Na (**2**), K (**3**) and Cs (**4**) and to $A_{0.5}UNbO_{5.75}$, for $A = Rb$ (**5**) and Cs (**6**). For all compounds, cell parameters were refined from powder X-ray diffraction data, using Rietveld method and Fullprof program [49]. Using single crystal results for $LiUNbO_6$, the powder X-ray diffraction pattern of **1** is unambiguously indexed with a monoclinic unit cell and refined parameters $a_1 = 10.3087(8)$, $b_1 = 6.4214(6)$, $c_1 = 7.6553(6)$ Å, $\beta_1 = 101.18(1)^\circ$. In accordance with the single crystal results, the powder X-ray diffraction data of **3**, **5** and **6** are unambiguously indexed with an orthorhombic unit cell parameters with refined parameters ($a_3 = 10.2537(2)$, $b_3 = 7.5788(1)$, $c_3 = 13.3824(2)$Å; $a_5 = 10.4270(5)$, $b_5 = 7.6585(3)$, $c_5 = 13.3824(2)$Å and $a_6 = 13.7674(8)$, $b_6 = 10.6157(6)$, $c_6 = 7.6912(4)$ Å) for **3**, **5** and **6**, respectively. Indexation of powder X-ray diffraction patterns indicates a *B*-lattice for **6** and a *P*-lattice **3** and **5**. For compound **4**, both powder and single crystal X-ray diffraction data indicated that this compound adopt the layered crystal structure reported by Gasperin [45].

For $M = Li$, K, single crystals of formula $MUNbO_6$, 1 and 3, were obtained whatever the starting stoichiometry. For $M = Rb$, for the starting compositions, crystals of $Rb_{0.5}UNbO_{5.75}$ (**5**) were grown. For $M = Cs$, two types of single crystals corresponding to $Cs_{0.5}UNbO_{5.75}$ (**6**) and $CsUNbO_6$ (**4**) were isolated from the corresponding stoechiometric starting mixtures. Except for **2**, unit cell parameters of the isolated single crystals correspond to those of the prepared powder. In fact, the single crystal obtained for the composition corresponding to **2** gave a unit cell similar to that of the K-compound **3**. An energy dispersive spectroscopy (EDS) analysis on the single crystal used for the structure determination revealed the presence, in more of the expected elements, of Cs in a small quantity from the furnace contaminated by the previous experiments using cesium carbonate. This result will be discussed in the appropriate section. For all other crystals, EDS analysis indicate only the chemical elements used at the beginning of each reaction.

In the absence of single crystal structure determination and known cell parameters for the sodium compound **2**, about 20 pattern peak positions are extracted with the *Topas P* of *BRUKER-DIFFRAC*^{plus} software package, and used to determine cell parameters. To obtain peak positions with the maximum of precision each reflection profile was refined using the pseudo-Voigt function. The cell parameters were obtained by combination the indexing programs TREOR [50] and DICVOL [51,52], using all extracted reflections. Thus, the X-ray diagram of this phase has been indexed and refined in a monoclinic system with cell parameters and indexed reflections given in Table 1.

Table 1
X-ray powder pattern of $NaUNbO_6$

hkl	2θ	*I*(%)	*hkl*	2θ	*I* (%)
110	14.670	22	−432	49.002	11
200	14.886	47	132	49.290	82
111	21.480	22	−604	51.177	2
−112	26.133	27	−713	51.541	1
120	26.522	15	−623	51.720	14
−401	26.654	10	004	51.845	6
−121	27.890	4	−224	53.764	2
−312	28.052	36	−802	54.905	3
012	28.329	14	−803	55.998	2
220	29.588	100	−721	56.019	2
−411	29.597	85	104	56.114	7
400	30.031	11	332	57.775	2
311	33.124	16	−624	57.989	2
−203	33.979	3	241	58.045	2
320	34.142	12	−305	58.549	82
−303	34.291	26	323	60.267	1
−222	34.320	28	440	61.420	15
−122	34.397	3	−822	61.439	3
−213	36.387	2	−821	63.511	1
−601	41.248	1	−705	63.546	5
103	42.463	2	−443	65.230	1
222	43.765	7	−901	65.594	1
113	44.479	3	−634	65.856	7
330	45.042	5	−625	66.866	1
501	45.450	1	−911	67.108	2
−304	45.744	3	−923	68.983	3
520	46.100	5	143	69.491	1
−613	46.201	9	541	71.690	2
−404	46.291	2	−606	72.257	4
−204	46.532	4	−335	72.310	3
032	46.642	2	−432	49.002	11

$NaUNbO_6$: $a = 13.3777(5)$ Å, $b = 7.0010(2)$ Å, $c = 7.9282(2)$ Å and $\beta = 117.25(1)^\circ$.

3.2. Structure refinement and solution

Systematic absences of reflections were consistent with $P2_1/c$ centro-symmetric space group for **1**. The measured density indicated $Z = 4$ formula per unit cell with $\rho_{mes} = 5.80(3)$ and $\rho_{calc} = 5.84(2)\,g\,cm^{-3}$ calculated for $LiUNbO_6$.

For **3**, **5** and **7**, systematic absences of reflections were consistent with *Pnma* centro-symmetric space group. The densities calculated for the formula $KUNbO_6$ and $Rb_{0.5}UNbO_{5.75}$ with $Z = 8$ and 4 formula per unit cell, 5.91(1) and 5.57(3) $g\,cm^{-3}$, respectively, are in good agreement with the measured values, $\rho_{mes} = 5.93(3)$ and 5.54(5) $g\,cm^{-3}$.

Finally, for **6**, the crystal structure was solved in *Cmcm* space group. The cell parameters are also reported in the non-conventional *Bbmm* space group for comparison. The measured density, 5.65(3) $g\,cm^{-3}$, is in good accordance with the calculated value considering $Z = 4$ formula $Cs_{0.5}UNbO_{5.75}$ per unit cell, 5.67(1) $g\,cm^{-3}$.

The structures were solved in the above centro-symmetric space groups and in the last cycles of refinement atomic coordinates and anisotropic displacement parameters were refined for all atoms, except Li in **1** for which an isotropic displacement parameter was used. For **5**, the Rb alkaline metal site is half-occupied. For **5** and **6**, oxygen sites, O(9) and O(5), respectively, are three-quarters occupied leading to acceptable displacement parameters and achieving electro-neutrality. Relevant crystallographic information is compiled in Tables 2 and 3 for AUNbO$_6$ and $A_{0.5}$UNbO$_{5.75}$ compounds, respectively. The final atomic positions with isotropic (for Li in **1**) or equivalent displacement parameters are presented in Table 4 for **1**, in Table 5 for **3**, **7** and **4**, and in Table 6 for **6**.

4. Description of the crystal structures

4.1. $LiUNbO_6$

Selected interatomic distances for LiUNbO$_6$ with the uranyl ion angle, and bond valence sums calculated using Burns et al. data [53] for U–O bonds and Brese and O'Keeffe parameters [54] for the other bonds, are reported in Table 7.

The crystal structure of LiUNbO$_6$ is built from an assemblage of NbO$_6$ distorted octahedra and UO$_7$ pentagonal bipyramids to give a two-dimensional arrangement. The only independent uranium atom is bonded to O(1) and O(2) atoms at short distances of 1.837(11) and 1.811(12) Å,

Table 2
Crystal data, intensity collection and structure refinement parameters for the AUNbO$_6$ compounds A = Li (**1**), K (**3**) and Na$_{0.92}$Cs$_{0.08}$ (**7**)

	1		**3**		**7**	
Crystal data						
Crystal symmetry	Monoclinic		Orthorhombic		Orthorhombic	
Space group	$P2_1/c$		*Pnma*		*Pnma*	
Unit cell refined from	$a = 10.3091(11)$		10.307(2)		10.272(4)	
Single crystal data (Å)	$b = 6.4414(10)$		7.588(1)		7.628(3)	
	$c = 7.5602(5)$		13.403(2)		13.451(5)	
	$\beta = 100.65(1)^\circ$					
Unit cell volume (Å^3)	493.4(3)		1048.3(3)		1053.9(7)	
Z	4		8		8	
Calculated density (g cm^{-3})	5.84(2)		5.91(1)		5.78(1)4	
Measured density (g cm^{-3})	5.80(3)		5.93(3)			
Data collection						
Temperature (K)	293(2)		293(2)		293(2)	
Equipment	Bruker SMART		Bruker SMART		Bruker SMART	
Radiation Mo$K\alpha$ (Å)	0.71073		0.71073		0.71073	
Scan mode	ω		ω		ω	
Recording θ min/max (deg)	3.75/29.04		2.49/23.33		2.49/30.03	
Recording reciprocal space	$-13 \leqslant h \leqslant 13$		$-11 \leqslant h \leqslant 11$		$-14 \leqslant h \leqslant 13$	
	$-8 \leqslant k \leqslant 8$		$-8 \leqslant k \leqslant 8$		$-10 \leqslant k \leqslant 10$	
	$-9 \leqslant l \leqslant 10$		$-14 \leqslant l \leqslant 14$		$-18 \leqslant l \leqslant 18$	
No. of measured reflections	3104		5420		5066	
R merging factor	0.050		0.057		0.066	
No. of independent reflections	1149		723		792	
μ (cm^{-1})	350.47		337.88	334.37		
Crystal faces and distances (mm)	$13\bar{1}$	0.106	100	0.038	100	0.029
From an arbitrary origin	$\bar{1}\bar{3}1$	0.106		0.038	$\bar{1}00$	0.029
	$\bar{3}21$	0.116	010	0.047	010	0.057
	$3\bar{2}\bar{1}$	0.116		0.047	$0\bar{1}0$	0.057
	001	0.018	001	0.019	001	0.021
	$00\bar{1}$	0.018	$00\bar{1}$	0.019	$00\bar{1}$	0.021
	$\bar{5}\bar{1}1$	0.190				
Refinement						
Refined parameters/restraints	72/0		95/0		96/0	
Goodness of fit on F^2	1.06		1.12		1.14	
R_1 for all data	0.053		0.023		0.036	
wR_2 for all data	0.107		0.058		0.088	
Largest diff. peak and hole (e Å^{-3})	2.22/−2.56		1.71/−1.94		3.50/−2.01	
CSD number	416590		416589		**416591**	

$R_1 = \Sigma(|F_o| - |F_c|)/\Sigma|F_o|$.
w$R_2 = [\Sigma w(F_o^2 - F_c^2)^2/\Sigma w(F_o^2)^2]^{1/2}$.
$w = 1/[\sigma^2(F_0^2) + (aP)^2 + bP]$ where a and b are refined parameters and $P = (F_o^2 + 2F_c^2)/3$.

Table 3
Crystal data, intensity collection and structure refinement parameters for the $A_{0.5}NbUO_{5.75}$ compounds, A = Rb (**5**) and Cs (**6**)

	5		6	
Crystal data				
Crystal symmetry	Orthorhombic		Orthorhombic	
Space group	*Pnma*		*Cmcm*	*or Bbmm*
Unit cell refined from	$a = 10.432(3)$		13.952(3)	10.607(2)
single crystal data (Å)	$b = 7.681(2)$		10.607(2)	7.748(2)
	$c = 13.853(4)$		7.748(2)	13.952(3)
Unit cell volume (Å^3)	1110.0(5)		1146.6(4)	
Z	8		8	
Calculated density (g cm^{-3})	5.57(3)		5.67(1)	
Measured density (g cm^{-3})	5.54(5)		5.65(3)	
Data collection				
Temperature (K)	293(2)		293(2)	
Equipment	Bruker SMART		Bruker SMART	
Radiation Mo$K\alpha$ (Å)	0.71073		0.71073	
Scan mode	ω		ω	
Recording θ min/max (deg)	3.53/29.29		2.92/29.97	
Recording reciprocal space	$-13 \leqslant h \leqslant 14$		$-19 \leqslant h \leqslant 19$	
	$-10 \leqslant k \leqslant 10$		$-14 \leqslant k \leqslant 14$	
	$-18 \leqslant 1 \leqslant 18$		$-10 \leqslant l \leqslant 10$	
No. of measured reflections	7693		4311	
R merging factor	0.067		0.059	
No. of independent reflections	1406		668	
μ (cm^{-1})	355.05		332.85	
Limiting faces and distances (mm)	1 0 0	0.080	1 0 0	0.044
From an arbitrary origin	$\bar{1}$ 0 0	0.080	$\bar{1}$ 0 0	0.044
	0 1 0	0.023	0 1 0	0.032
	0 $\bar{1}$ 0	0.023	0 $\bar{1}$ 0	0.032
	0 $\bar{2}$ 1	0.052	0 0 1	0.015
	0 2 $\bar{1}$	0.052	0 0 $\bar{1}$	0.015
Refinement				
Refined parameters/restraints	94/0		49/0	
Goodness of fit on F^2	1.06		1.23	
R_1 for all data	0.046		0.044	
wR_2 for all data	0.106		0.117	
Largest diff. peak and hole(e Å^{-3})	3.17/−3.96		3.05/−2.60	
CSD number	416592		416588	

$R_1 = \Sigma(|F_o|-|F_c|)/\Sigma|F_o|$.
$wR_2 = [\Sigma w(F_o^2-F_c^2)^2/\Sigma w(F_o^2)^2]^{1/2}$.
$w = 1/[\sigma^2(F_0^2) + (aP)^2 + bP]$ where a and b are refined parameters and $P = (F_o^2 + 2F_c^2)/3$.

Table 4
Atomic positions with equivalent or isotropic displacements parameters for $LiNbUO_6$

Atom	Site	x	y	z	U_{eq}^a/U_{iso}^b (Å^2)
U	4*e*	0.68978(4)	0.19987(7)	0.92032(5)	0.0094(2)
Nb	4*e*	0.72686(12)	0.75018(19)	0.68036(15)	0.0101(2)
Li	4*e*	0.008(5)	0.987(8)	0.832(7)	0.075(13)[b]
O(1)	4*e*	0.8706(11)	0.1804(14)	0.9711(16)	0.016(2)
O(2)	4*e*	0.5113(12)	0.2145(14)	0.8696(15)	0.016(2)
O(3)	4*e*	0.6908(9)	0.8267(17)	0.9214(12)	0.014(2)
O(4)	4*e*	0.6947(9)	0.0454(14)	0.6335(13)	0.014(1)
O(5)	4*e*	0.7028(9)	0.4491(14)	0.7129(12)	0.014(2)
O(6)	4*e*	0.9028(11)	0.7505(18)	0.7250(16)	0.016(2)

Note: [a]The U_{eq} values are defined by $U_{eq} = 1/3(\sum_i \sum_j U_{ij} a^*_i a^*_j a_i a_j)$.
[b]U_{iso} for Li atom.

Table 5
Atomic positions with equivalent thermal displacements for AUNbO$_6$ compounds A = K (**3**, first line, bold), Na$_{0.92}$Cs$_{0.08}$ (**7**, second line, italic) and Rb$_{0.5}$UNbO$_{5.75}$ (**5**, third line)

Atom	Site.	Occ.	x	y	z	U_{eq} (Å^2)
U(1)	4*c*	**1**	**0.31533(5)**	**1/4**	**0.70083(4)**	**0.0103(2)**
		1	*0.31347(10)*	*1/4*	*0.70132(8)*	*0.0136(3)*
		1	0.29736(6)	1/4	0.70998(4)	0.0143(2)
U(2)	4*c*	**1**	**0.35526(5)**	**3/4**	**0.72634(4)**	**0.0104(2)**
		1	*0.35311(10)*	*3/4*	*0.72684(8)*	*0.0137(3)*
		1	*0.33863(6)*	*3/4*	*0.73780(4)*	*0.0150(2)*
Nb	8*d*	**1**	**0.05063(9)**	**0.00073(11)**	**0.61061(8)**	**0.0134(3)**
		1	*0.04845(15)*	*0.0009(2)*	*0.60876(11)*	*0.0066(3)*
		1	0.04310(9)	0.00064(10)	0.61364(8)	0.0154(2)
K		**1**	**0.3589(3)**	**0.9892(3)**	**0.4424(2)**	**0.027(1)**
Na/Cs		0.92(1)/0.08(1)	*0.3619(7)*	*0.9885(8)*	*0.4422(5)*	*0.035(3)*
Rb	8*d*	0.5	0.3872(3)	0.9804(3)	0.4571(2)	0.0300(5)
O(1)	4*c*	**1**	**0.2487(9)**	**3/4**	**0.8316(8)**	**0.015(2)**
		1	*0.2458(17)*	*3/4*	*0.8295(15)*	*0.020(5)*
		1	0.2341(12)	3/4	0.8408(9)	0.024(3)
O(2)	4*c*	**1**	**0.4105(10)**	**1/4**	**0.5883(8)**	**0.018(2)**
		1	*0.4094(18)*	*1/4*	*0.5884(15)*	*0.025(5)*
		1	0.3942(11)	1/4	0.6012(8)	0.022(2)
O(3)	4*c*	**1**	**0.1062(9)**	**1/4**	**0.6150(7)**	**0.011(2)**
		1	*0.1044(19)*	*1/4*	*0.6121(14)*	*0.015(4)*
		1	0.0975(10)	1/4	0.6196(8)	0.020(2)
O(4)	4*c*	**1**	**0.4544(9)**	**3/4**	**0.6159(7)**	**0.017(2)**
		1	*0.4557(19)*	*3/4*	*0.6175(15)*	*0.026(5)*
		1	0.4405(12)	3/4	0.6320(8)	0.025(3)
O(5)	8*d*	**1**	**0.9440(7)**	**0.0341(9)**	**0.7310(5)**	**0.013(1)**
		1	*0.9427(12)*	*0.0338(16)*	*0.7303(10)*	*0.015(3)*
		1	0.9256(7)	0.0353(9)	0.7212(5)	0.017(2)
O(6)	4*c*	**1**	**0.2186(10)**	**1/4**	**0.8119(7)**	**0.016(2)**
		1	*0.216(2)*	*1/4*	*0.8104(14)*	*0.022(4)*
		1	0.2014(12)	1/4	0.8166(8)	0.025(3)
O(7)	8*d*	**1**	**0.2316(6)**	**0.9692(8)**	**0.6570(6)**	**0.014(1)**
		1	*0.2293(13)*	*0.9686(15)*	*0.6596(11)*	*0.018(3)*
		1	0.2140(7)	0.9676(10)	0.6687(6)	0.017(2)
O(8)	4*c*	**1**	**0.0182(9)**	**3/4**	**0.6438(8)**	**0.014(2)**
		1	*0.0154(16)*	*3/4*	*0.6422(15)*	*0.017(4)*
		1	0.0067(10)	3/4	0.6418(7)	0.017(2)
O(9)	8*d*	**1**	**0.8930(8)**	**0.0513(11)**	**0.5273(6)**	**0.020(3)**
		1	*0.8941(13)*	*0.0454(19)*	*0.5256(11)*	*0.026(3)*
		0.75	0.8933(10)	0.0565(17)	0.5201(8)	0.028(3)

Note: The U_{eq} values are defined by $U_{eq} = 1/3(\sum_i\sum_j U_{ij}a^*_i a^*_j a_i a_j)$.

respectively, forming a nearly linear uranyl UO_2^{2+} ion, 179.1(5)°. The uranyl ion is further coordinated by five equatorial oxygen atoms at distances in the range 2.265(9)–2.404(11) Å to give a pentagonal bipyramidal environment. The UO_7 bipyramids share the opposite O(4)–O(5) equatorial edges, creating infinite $^1_\infty[UO_5]^{4-}$ chains running down [001], Fig. 1a. Such infinite chains are observed in many uranyl oxides, where the chains are connected by various ways, as for example, in the previously reported compounds UVO_5 [29–31], $USbO_5$ [55], UMo_2O_8 [56], $U_2P_2O_{10}$ [57], and in other recently studied compounds like uranyl divanadate, $(UO_2)_2V_2O_7$ [58,59], pentahydrated uranyl orthovanadate $(UO_2)_3(VO_4)_2\cdot 5H_2O$ [23], $A_6(UO_2)_5(VO_4)_2O_5$ with A = Na, K, Rb [22,24], $K_2(UO_2)W_2O_8$ [16,17] and $Li_2UO_2(WO_4)_2$ [19]. The topological studies of uranyl compounds [60,61] show the importance of these $^1_\infty[UO_5]^{4-}$ chains in the structure of numerous uranyl compounds. The only independent niobium atom presents a very distorted octahedral environment of oxygen atoms, with four atoms at distances

Table 6
Atomic positions with equivalent thermal displacements $Cs_{0.5}NbUO_{5.75}$

Atom	Site	Occ.	x	y	z	U_{eq} (Å^2)
U	8*g*	1	0.23657(6)	0.27029(8)	1/4	0.0167(3)
Nb	8*e*	1	0.11466(15)	1/2	0	0.0125(4)
Cs	4*a*	1	1/2	1/2	0	0.0618(9)
O(1)	16*h*	1	0.2010(9)	0.3554(11)	0.9668(14)	0.023(3)
O(2)	8*g*	1	0.1354(11)	0.4523(16)	1/4	0.018(3)
O(3)	8*g*	1	0.1324(15)	0.1723(17)	1/4	0.032(4)
O(4)	8*g*	1	0.3414(13)	0.3663(17)	1/4	0.025(4)
O(5)	8*f*	0.75	0	0.609(2)	0.054(4)	0.031(6)

Note: The U_{eq} values are defined by $U_{eq} = 1/3(\sum_i \sum_j U_{ij} a^*_i a^*_j a_i a_j)$.
The crystal structure was solved in *Cmcm* space group.

Table 7
Bond distances (Å), bond valences *Sij* and uranyl angles (deg) in $LiNbUO_6$

U environment					
	d_{U-O}	S_{ij}			
U–O(2)	1.811(12)	1.585	Uranyl angles (deg)		
U–O(1)	1.837(11)	1.513	O(2)–U–O(1)	179.1(5)	
U–O(5)	2.265(9)	0.661			
U–O(4)^{i}	2.294(9)	0.626			
U–O(5)^{i}	2.392(9)	0.518			
U–O(4)	2.395(11)	0.515			
U–O(3)^{ii}	2.404(11)	0.507			
	$\sum S_{ij}$	5.925			
Nb octahedral environment			*Li environment*		
	d_{Nb-O}	S_{ij}	d_{Li-O}		S_{ij}
Nb–O(6)	1.783(11)	1.417	Li–O(6)^{vii}	1.96(5)	0.263
Nb–O(4)^{iv}	1.951(9)	0.895	Li–O(6)^{vi}	2.02(5)	0.230
Nb–O(5)	1.976(9)	0.839	Li–O(1)^{iii}	2.06(5)	0.201
Nb–O(3)^{v}	1.987(9)	0.814	Li–O(1)^{viii}	2.28(6)	0.111
Nb–O(3)	1.988(10)	0.812			
Nb–O(2)^{vi}	2.425(12)	0.249			
	$\sum S_{ij}$	5.026		$\sum S_{ij}$	0.805

Symmetry codes: (i) x, $0.5-y$, $0.5+z$; (ii) x, $-1+y$, z; (iii) $1-x$, $1-y$, $2-z$; (iv) x, $1+y$, z; (v) x, $1.5-y$, $-0.5+z$; (vii) $1-x$, $0.5+y$, $1.5-z$; (xii) $-1+x$, y, z; (viii) $-1+x$, $1+y$, z.

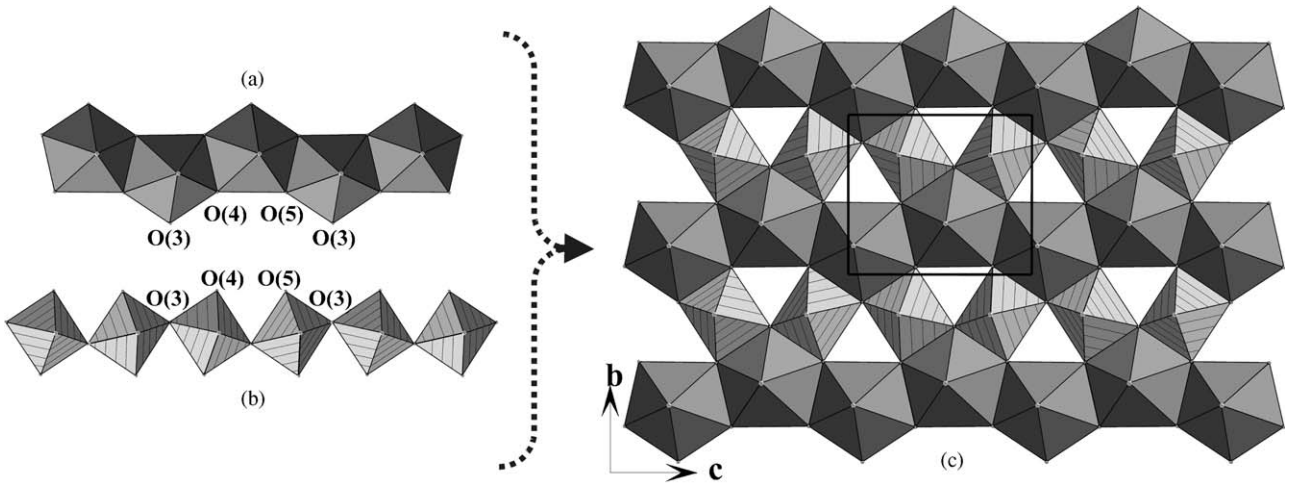

Fig. 1. The layer $^{2}_{\infty}[(UO_2)(NbO)O_3]^{-}$ in $LiNbUO_6$ (c) built by edge sharing between $^{1}_{\infty}[UO_5]^{4-}$ chains of edge-shared UO_7 pentagonal bipyramids (a) and $^{1}_{\infty}[NbO_4]^{3-}$ chains of corner-shared NbO_5 square pyramids (b).

from 1.951(9) to 1.988(10) Å forming a square and two axial oxygen atoms at shorter and longer distances, 1.783(11) and 2.425(12) Å, respectively; so the coordination of Nb approximates to square pyramidal. Each NbO_5 square pyramid shares equatorial corners O(3) with two adjacent pyramids to form a chain $^1_\infty[NbO_4]^{3-}$ running down [001], Fig. 1b. Thus $^2_\infty[(UO_2)(NbO)O_3]^-$ layers are formed by the association by edge sharing of these two types of chains alternating along [010], Fig. 1c. The resulting layers are of uranophane sheet anion topology [60,61], where pentagons are occupied by U and squares by Nb. Two consecutive layers at $x\sim0.3$ and ~0.7 related by a center of symmetry form a double sheet, Fig. 2a. The Li^+ ions are located in the available space between successive double layers and are found to be at the centers of nearly regular tetrahedra of oxygen atoms. Thus, the $LiUNbO_6$ structure results from the stacking of neutral sandwiches of $\{(UNbO_6)^-$–$(Li)_2^{2+}$–$(UNbO_6)^-\}$, of Li^{2+} layers between two $UNbO_6^-$ uranyl niobate sheets, Fig. 2a. The bonds between the neutral sandwiches are very weak, they correspond to the formation of weak Nb–O bonds, with Nb–O distance of 2.425(12) Å, involving oxygen of uranyl ions and leading to a distorted octahedral environment of Nb atoms. The contribution of the O(2) atom to the valence bond sum of Nb is 0.25 v.u.

Bond valence sums calculation provides values of 5.93, 5.03 and 0.81 for U, Nb, and Li, respectively, which are consistent with formal valences U^{6+}, Nb^{5+} and Li^+. For oxygen atoms the calculated valence bond sums ranged from 1.83 to 2.13 with an average value of 1.96, showing that the oxygen atoms are only in the O^{2-} ion oxide form.

It is interesting to compare the structure of $LiUNbO_6$ with those of UMO_5 (M = Mo, Sb, V, Nb) compounds, which contain U^{4+} (M = Mo) [62] or U^{5+} (M = Sb, V, Nb) [29–31,55]. In these compounds, $(UO_5)_\infty$ chains share edges with square bases of MO_6 distorted octahedra resulting in layers of uranophane sheet anion topology [60,61] that are stacked by perpendicular chains containing–U–O–U–O–and–M–O–M–O–for M = Mo, V, Nb, and heterometallic– U–O–Sb–O–U–O–Sb–O–in $USbO_5$. In these compounds with pillared layer structure, no uranyl group is present, the U–O bond lengths along the chains perpendicular to the layers are greater than 2.0 Å. One can imagine that $LiUNbO_6$ structure can be deduced from $USbO_5$ [55] (Fig. 2b), by the replacement of U^{5+} by U^{6+} leading to the formation of uranyl bonds and by the separation of two successive sheets once on two to create interspace occupied by the alkaline ions. In some cases, all the layers are separated by alkaline metals to form monolayered structures. Thus, the layered structure of the $AUNbO_6$ (A = K, Rb) compounds reported by Gasperin et al. [44] is obtained, in which A atoms occupy all the spaces between consecutive $^2_\infty[(UO_2)(NbO)O_3]^-$ layers, Fig. 2c. However, it is noticed that in $LiUNbO_6$ the apical NbO bands of one layer are all oriented above the layer, while in $AUNbO_6$ (A = K, Rb) they alternate above and below the layer for successive chains leading to corrugated layers.

4.2. $AUNbO_6$, A = K, (Na, Cs)

Selected interatomic distances with uranyl ion angles, and bond valence sums for **3** and **7** are reported in Table 8.

The crystal structure of $KUNbO_6$ determined by the present study contains two independent uranium atoms, U(1) and U(2) in particular positions (4*c*). The local environment about each uranium is a pentagonal bipyramid, with shorter axial bonds in the range 1.788(9)–1.799(11) Å and longer equatorial bonds in the larger range 2.292(6)–2.443(9) Å, typical of UO_2^{2+} uranyl ion. The equatorial mean bond lengths of 2.357(2) and 2.365(2) Å for $U(1)O_2^{2+}$ and $U(2)O_2^{2+}$, respectively, are in excellent agreement with the average bond length of 2.37 Å determined by Burns et al. [53] for uranyl ions in pentagonal bipyramidal coordination from numerous well refined structures. U(1) and U(2) alternate in $^1_\infty[UO_5]^{4-}$ chains similar to that found in $LiUNbO_6$ and running down [010], Fig. 3a. There is one independent niobium atom in an octahedral environment of oxygen atoms with distances in the range 1.969(7)–2.008(8) Å. Two NbO_6

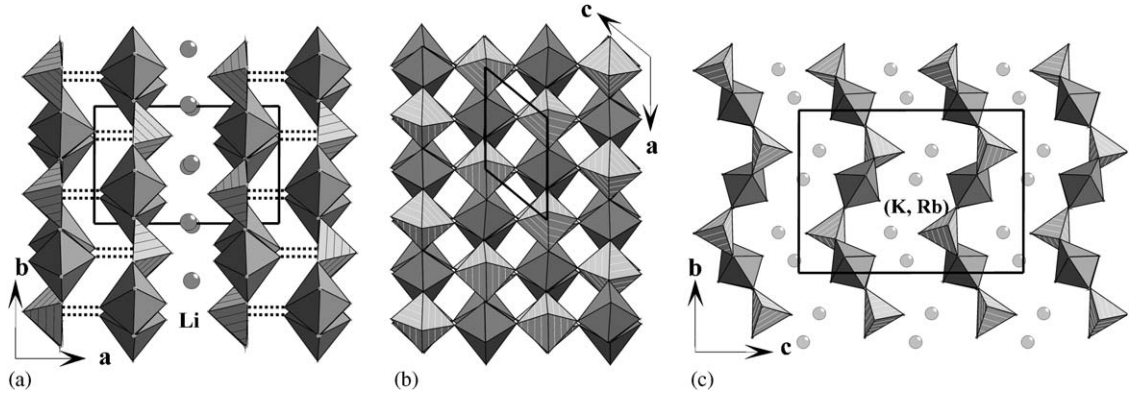

Fig. 2. Comparison of the structures of $LiNbUO_6$ (a), $USbO_5$ (b) and $ANbUO_6$ (A = K, Rb) (c), built from the same type of layers that are pillared in $USbO_5$ (b), separated once on two by Li^+ in $LiNbUO_6$ (a) and all separated by alkaline cation A^+ in $ANbUO_6$ compounds as reported by Gasperin [42] (c) The orientation of successive NbO_5 pyramids leads to planar layers in $LiNbUO_6$ and to corrugated layers in $ANbUO_6$ (A = Rb, Cs).

Table 8
Bond distances (Å), bond valences S_{ij} and uranyl angles (deg) in $AUNbO_6$ compounds with $A = K$ (**3**), $Na_{0.92}Cs_{0.08}$ (**7**), and in $Rb_{0.5}UNbO_{5.75}$ (**5**)

	(**3**)		(**7**)		(**5**)	
U environment	d_{U-O}	S_{ij}	d_{U-O}	S_{ij}	d_{U-O}	S_{ij}
U(1)–O(6)	1.792(10)	*1.650*	1.776(19)	1.718	1.784(12)	*1.673*
U(1)–O(2)	1.799(11)	*1.622*	1.811(20)	1.588	1.814(11)	*1.579*
U(1)–O(5)^{i}	2.297(7)	*0. 623*	2.308(12)	0.609	2.328(7)	*0.586*
U(1)–O(5)^{ii}	2.297(7)	*0. 623*	2.308(12)	0.609	2.328(7)	*0.586*
U(1)–O(7)^{iii}	2.373(6)	*0. 538*	2.381(12)	0.529	2.406(8)	*0.505*
U(1)–O(7)^{iv}	2.373(6)	*0. 538*	2.381(12)	0.529	2.406(8)	*0.505*
U(1)–O(3)	2.443(9)	*0. 470*	2.460(20)	0.455	2.432(11)	*0.480*
$\sum\sigma_{\varphi 1}$		*6.064*		6.037		*5.914*
U(2)–O(1)	1.788(9)	*1.663*	1.768(19)	1.728	1.796(13)	*1.634*
U(2)–O(4)	1.799(9)	*1.625*	1.809(20)	1.591	1.810(12)	*1.591*
U(2)–O(7)^{iv}	2.292(6)	*0. 629*	2.284(13)	0.638	2.324(8)	*0.591*
U(2)–O(7)	2.292(6)	*0. 629*	2.284(13)	0.638	2.324(8)	*0.591*
U(2)–O(5)^{i}	2.411(7)	*0. 500*	2.422(13)	0.489	2.420(15)	*0.491*
U(2)–O(5)^{v}	2.411(7)	*0. 500*	2.422(13)	0.489	2.420(15)	*0.491*
U(2)–O(8)^{vi}	2.419(9)	*0. 492*	2.425(19)	0.486	2.439(7)	*0.474*
$\sum\sigma_{\varphi 1}$		*6.038*		6.059		*5.846*
Nb environment	d_{Nb-O}	S_{ij}	d_{Nb-O}	S_{ij}	d_{Nb-O}	S_{ij}
Nb–O(5)^{viii}	1.969(7)	*0.855*	1.979(14)	*0.832*	1.948(7)	*0.905*
Nb–O(3)	1.977(8)	*0.837*	1.986(6)	*0.817*	1.999(3)	*0.788*
Nb–O(7)^{iii}	1.977(3)	*0.837*	1.995(14)	*0.797*	1.956(8)	*0.885*
Nb–O(9)^{ix}	1.977(3)	*0.837*	1.970(14)	*0.853*	2.016(3)	*0.753*
Nb–O(8)^{iii}	1.982(3)	*0.825*	1.995(6)	*0.797*	2001(3)	*0.784*
Nb–O(9)^{viii}	2.008(8)	*0.767*	1.934(15)	*0.940*	2.075(8)	*0.642*
$\sum\sigma_{\varphi 1}$		*4.949*		*5.036*		*4.757*
A environment	d_{K-O}	S_{ij}	d_{NaCs-O}	S_{ij}	d_{Rb-O}	S_{ij}
A–O(6)^{x}	2.644(7)	*0.250*	2.663(15)	0.097	2.788(9)	*0.241*
A–O(9)^{xi}	2.646(9)	*0.250*	2.678(15)	0.094	2.957(11)	*0.153*
A–O(1)^{xii}	2.711(7)	*0.209*	2.738(16)	0.079	2.913(9)	*0.173*
A–O(2)^{vii}	2.833(8)	*0.151*	2.843(16)	0.060	2.877(8)	*0.190*
A–O(4)^{xiii}	2.869(7)	*0.136*	2.852(16)	0.058	3.007(9)	*0.134*
A–O(2)^{viii}	3.019(9)	*0.091*	3.000(16)	0.039	2.997(10)	*0.137*
A–O(4)	3.110(8)	*0.071*	3.130(18)	0.028	3.051(9)	*0.119*
A–O(7)	3.165(8)	*0.061*	3.229(16)	0.021	3.445(8)	*0.041*
		1.219		0.476		*1.188*
Uranyl angles (deg)						
O(6)–U(1)–O(2)	179.2(5)		178.7(9)		179.7(5)	
O(1)–U(2)–O(4)	176.7(4)		177.0(9)		178.5(5)	

Symmetry codes: (i) $-0.5+x$, $0.5-y$, $1.5-z$; (ii) $-0.5+x$, y, $1.5-z$; (iii) x, $-1+y$, z; (iv) x, $1.5-y$, z; (v) $-0.5+x$, $1+y$, $1.5-z$; (vi) $0.5+x$, y, $1.5-z$; (vii) x, $1+y$, z; (viii) $1-x$, $-y$, $1-z$; (ix) $-1+x$, y, z; (x) $0.5-x$, $1-y$, $-0.5+z$; (xi) $1-x$, $1-y$, $1-z$; (xii) $0.5-x$, $2-y$, $-0.5+z$; (xiii) $1-x$, $2-y$, $1-z$.

octahedra share an O(9)–O(9) edge to form a dimeric unit, the dimeric units are further linked by corners to built a $^{1}_{\infty}[Nb_2O_8]^{6-}$ infinite ribbon, two octahedral wide, running down [010], Fig. 3b. The ribbons can also be considered as two chains of corner-shared octahedra, similar to those found in $LiUNbO_6$, connected by edges. The $^{1}_{\infty}[UO_5]^{4-}$ chains and the $^{1}_{\infty}[Nb_2O_8]^{6-}$ ribbons are associated by edge sharing to build a three-dimensional arrangement that creates large elliptic tunnels running down [010] and occupied by K atoms, Fig. 3c. The uranyl oxygen atoms point towards the center of the tunnels that can be described as formed by trigonal prism of uranyl oxygen atoms O(2)O(1)O(4)–O(4)O(6)O(2) associated first by a O(4)O(2)O(4)O(2) lateral square face and further by the trigonal faces O(1)O(2)O(4) and O(6)O(4)O(2). The K atoms occupy all the trigonal prisms and, to minimize the K^+–K^+ repulsion across the shared O(4)O(2)O(4)O(2) faces, they are displaced towards the O(4)O(2)O(4)O(2) lateral square face resulting in intra-dimer K^+–K^+ distance of 3.297(4) Å and an eight-fold coordination of K by oxygen atoms with K–O distances ranging from 2.644(7) to 3.165(8) Å, the oxygen O(9) and O(7) of a Nb_2O_8 dimer supplementing the alkaline trigonal prism environment to form a very distorted polyhedron, Fig. 4a.

On the basis of U–O, Nb–O and K–O distances, the calculated bond valence sums are 6.06 v.u. for U(1), 6.04 v.u. for U(2), 4.95 v.u. for Nb, and 1.22 v.u. for K, these values are consistent with formal valences of U^{6+}, Nb^{5+} and K^+. The bond valence sums for the O atoms are in the range from 1.79 to 2.15 v.u.

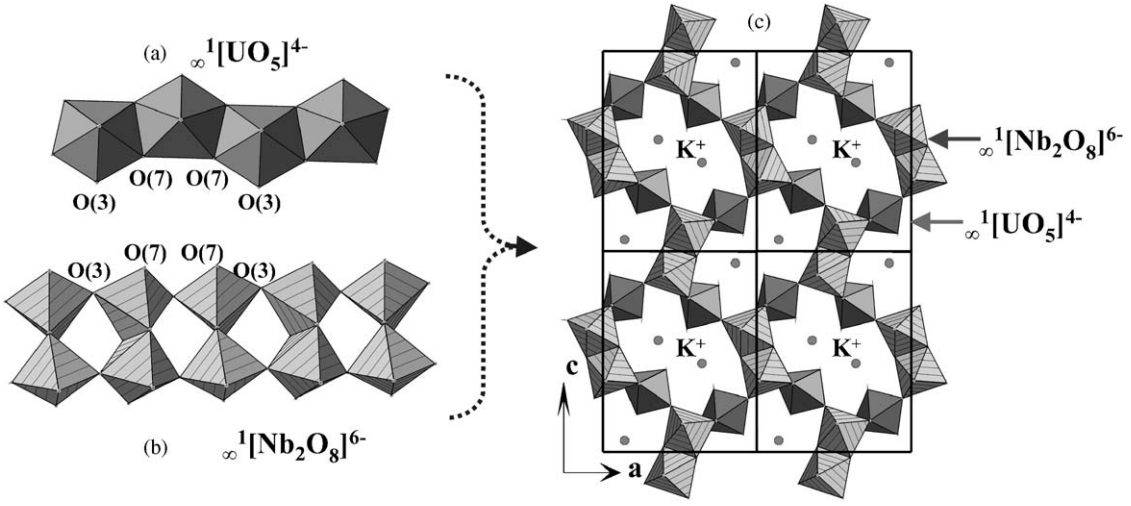

Fig. 3. $^1_\infty[UO_5]^{4-}$ chains of edge-shared UO_7 pentagonal bipyramids (a) and $^1_\infty[Nb_2O_8]^{6-}$ infinite ribbons, two octahedral wide (b), connected through edges to form a three-dimensional arrangement creating large elliptic tunnels running down the [010] and occupied by K^+ ions (c).

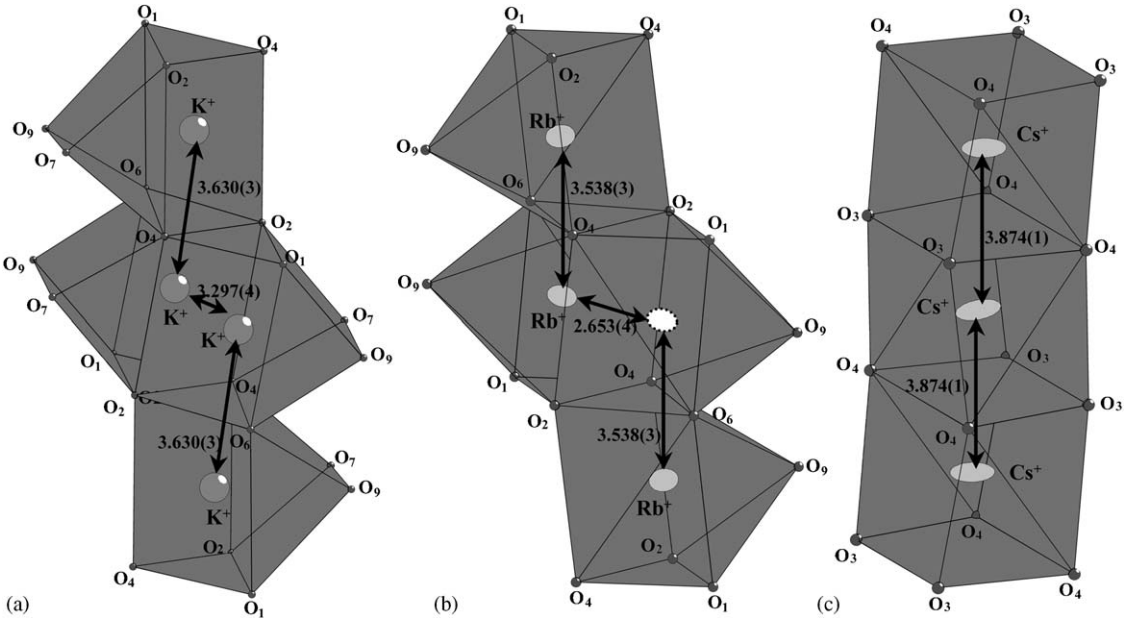

Fig. 4. In $KUNbO_6$ and $Rb_{0.5}UNbO_{5.75}$, the tunnels are formed by trigonal prisms of uranyl oxygen atoms O(2)O(1)O(4)–O(4)O(6)O(2) associated first by a O(4)O(2)O(4)O(2) lateral square face and further by the trigonal faces O(1)O(2)O(4) and O(6)O(4)O(2). The K atoms in occupy all the trigonal prisms and are displaced toward the O(4)O(2)O(4)O(2) lateral square face resulting in an eight-fold coordination of K (a). The Rb atoms occupy half the trigonal prisms and intra-tunnel disorder or intra-tunnel order (b) and inter-tunnel disorder can be imagined. In $Cs_{0.5}UNbO_{5.75}$, the tunnels are formed by columns of face-shared cubes of uranyl oxygen atoms (O(3)O(4))4 occupied by the Cs atoms (b).

For compound **7**, in agreement with the EDS results, the alkaline metal site was occupied both by Na and Cs, the occupation rate was refined to Na/Cs = 0.923(7)/0.077(7) leading to the crystallographic formula $Na_{0.92}Cs_{0.08}UNbO_6$. This mixed compound is isotypic with $KUNbO_6$. The Cs^+ ion plays a template role, which allows the construction of the uranyl niobate framework around this large cation. In fact, the tunnels are too large to accommodate little cations such as Na^+ only as shown by the too large Na–O distances leading to under-bonded ion revealed by the valence bond sum value calculated considering Na^+ only within the tunnels.

4.3. $A_{0.5}UNbO_{5.75}$, A = Rb (5), Cs (6)

Selected interatomic distances are reported in Tables 8 and 9, for **5** and **6**, respectively.

The structures of these compounds are built from the same type of three-dimensional arrangement of uranium and niobium polyhedra with different occupation of the

Table 9
Bond distances (Å), bond valences *Sij* and uranyl angles (deg) in $Cs_{0.5}UNbO_{5.75}$

U environment	d_{U-O}	S_{ij}			
U–O(4)	1.782(18)	1.679	Uranyl angles (deg)		
U–O(3)	1.787(20)	1.663	O(4)–U–O(3)	179.3(9)	
U–O(1)^{i}	2.315(11)	0.602			
U–O(1)^{ii}	2.315(11)	0.602			
U–O(2)	2.392(16)	0.518			
U–O(1)^{iii}	2.424(11)	0.487			
U–O(1)	2.424(11)	0.487			
	$\sum S_{ij}$	6.038			
Nb octahedral environment	d_{Nb-O}	S_{ij}	*Cs environment*	d_{Cs-O}	S_{ij}
Nb–O(1)^{vi}	1.967(12)	0.860	Cs–O(3)^{ix}	3.241(15)	0.108
Nb–O(1)	1.967(12)	0.860	Cs–O(3)^{i}	3.241(15)	0.108
Nb–O(5)^{vii}	2.018(14)	0.755	Cs–O(3)^{x}	3.241(15)	0.108
Nb–O(5)	2.018(14)	0.755	Cs–O(3)^{xi}	3.241(15)	0.108
Nb–O(2)^{viii}	2.023(5)	0.739	Cs–O(4)^{viii}	3.265(15)	0.101
Nb–O(2)	2.023(5)	0.739	Cs–O(4)	3.265(15)	0.101
	$\sum S_{ij}$	4.708	Cs–O(4)^{xii}	3.265(15)	0.101
			Cs–O(4)^{xiii}	3.265(15)	0.101
				$\sum S_{ij}$	0.836

Symmetry codes: **(i)** 0.5−*x*, 0.5−*y*, −*z*; **(ii)** 0.5−*x*, 0.5−*y*, 0.5+*z*; **(iii)** *x*, *y*, 0.5−*z*; **(iv)** 0.5−*x*, 0.5−*y*, 1−*z*; **(v)** −0.5+*x*, −0.5+*y*, *z*; **(vi)** *x*, 1−*y*, −*z*; **(vii)** −*x*, 1−*y*, −*z*; **(viii)** *x*, 1−*y*, −0.5+*z*; **(ix)** 0.5+*x*, 0.5+*y*, *z*; **(x)** 0.5−*x*, 0.5+*y*, 0.5−*z*; **(xi)** 0.5+*x*, 0.5−*y*, −0.5+*z*; **(xii)** 1−*x*, 1−*y*, −*z*; **(xiii)** 1−*x*, *y*, 0.5−*z*; **(xiv)** 1−*x*, 1−*y*, 0.5+*z*; **(xv)** 1−*x*, 1−*y*, −0.5+*z*.

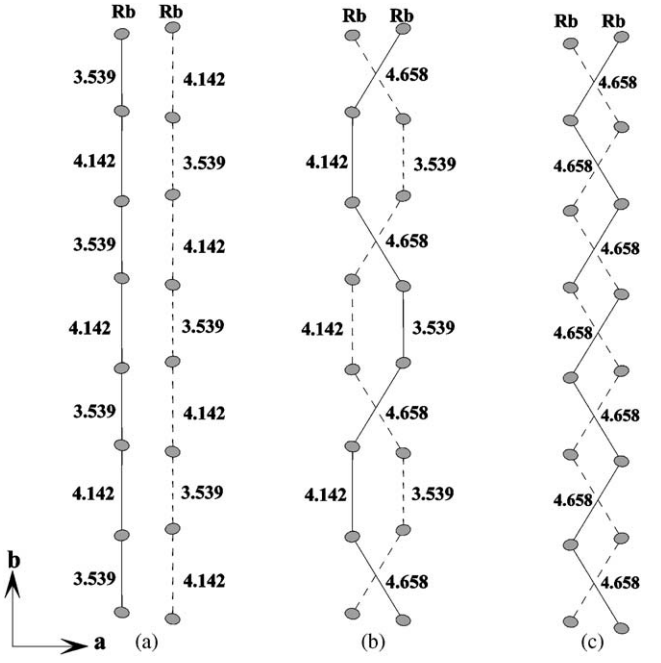

Fig. 5. Three possible intra-tunnel orders of rubidium atoms in $Rb_{0.5}UNbO_{5.75}$, with two possibilities for each case.

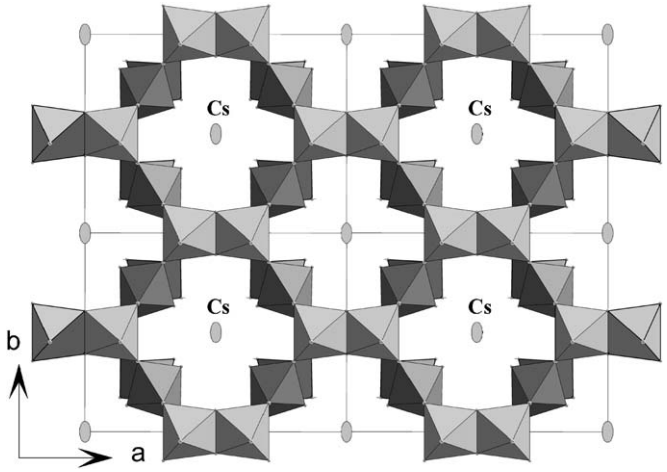

Fig. 6. Projection of the $Cs_{0.5}UNbO_{5.75}$ crystal structure in (001) showing the occupation of the cylindrical tunnels by Cs^{+} ions.

tunnels by alkaline metals. The rubidium compound is isostructural to $KUNbO_6$. The ionic radius of Rb^{+} ion does not allow the simultaneously occupation of all the (8*d*) sites, in fact they are half occupied. The two square face-shared trigonal prism forming the tunnels are never simultaneously occupied, so there is no more repulsion (the distance between an occupied and an empty site is 2.653(4) Å and Rb occupy nearly the center of a trigonal prism with a larger Rb–O(9) distance; furthermore, the O(7) atom does not participate to the Rb coordination which can be described as a mono-capped trigonal prism, Fig. 4b. Various order types can be imagined, an intra-tunnel ordering, with Rb–Rb distances of [3.539(3)–4.143(3) Å] Fig. 5a, [4.658(4)–4.143(3)–4.658(4)–3.539(3) Å] Fig. 5b, or more probably, an intra-tunnel ordering Rb–Rb distance of 4.658(4) Å, Fig. 5c, and an inter-tunnel disorder. No supplementary reflection indicates the existence of an inter-tunnel order. For $A = Tl$, the isotypic compound $Tl_{0.5}UNbO_{5.75}$ has been reported [44].

For the larger alkaline metal Cs, the polyhedral arrangement is more symmetric, Fig. 6, and tunnels with pseudo-square section are created, so the Cs atom is coordinated by eight uranyl oxygen atoms forming a slightly distorted cube. The tunnels can be described as a succession along [010] of face-shared CsO_8 cubes, Fig. 4c.

5. Discussion: the $A_{1-x}UMO_{6-x/2}$ (M = V, Nb) compounds, layered and tunneled structures

The various uranyl vanadate and uranyl niobate compounds reported for $x = 0$ and 0.5 are reported in Table 10. For M = V, $AUVO_6$ compounds exist for A = Na, K, Rb and Cs [39–43] as mineral or synthetic and adopt the carnotite-type layered structure in which V^{5+} is in a square pentagonal pyramidal coordination. Crystal structures of $LiUVO_6$ and $A_{0.5}UVO_{5.75}$ compounds have not been reported up to now. For M = Nb, the results are more conflicting. With A = Li and Na, previous attempts to prepare $AUNbO_6$ compounds by solid-state reaction were unsuccessful [63]; in fact, hydrated uranyl niobates $LiUNbO_6 \cdot 2H_2O$ and $NaUNbO_6 \cdot H_2O$ were obtained from $KUNbO_6$ by ion exchange, their thermal dehydration gave the anhydrous phases $AUNbO_6$. On the basis of unit cell parameters (Table 10) determined from X-ray powder diffraction data, compared to that of layered $KNbUO_6$ [44], layered structures have been announced [63]. For $LiUNbO_6$, the layered structure of the anhydrous compound has been confirmed in the present study, but with different lattice parameters. For $NaUNbO_6$, a different unit cell is obtained and ab-initio crystal structure determination is planned. With A = K and Rb, layered structure has been previously reported from X-ray single crystal diffraction study [44], but the author did not report the synthesis of the corresponding powders. Our attempts to prepare these compounds failed just as those of the monoclinic modification of $RbUNbO_6$ [64]; on the contrary, we obtain both powder and single crystals of $KUNbO_6$ and $Rb_{0.5}UNbO_{5.75}$ with similar tunneled structure. Finally, with A = Cs, the existence of a layered compound $CsUNbO_6$ with a carnotite-type uranyl-niobate layer described by Gasperin [45] has been confirmed in the present work; furthermore, a new tunneled compound $Cs_{0.5}UNbO_{5.75}$ has been obtained. These results show the complexity and interest of the crystal chemistry of the uranyl niobates and the key role of the alkaline cation on both connectivity and dimensionality of the obtained crystal structures. While Li occupy the inter-space between layers formed by the linkage of uranyl and niobium polyhedra, the larger K, Rb and Cs countercations lead to the formation of layers or frameworks. The cases of $Rb_{0.5}UNbO_{5.75}$ and $Cs_{0.5}UNbO_{5.75}$ are particularly instructional, the largest Cs cation directing the building of a more symmetrical framework around it. It is also noteworthy that the presence of a small quantity of Cs leads to the formation of the tunneled structure instead of the layered one as exemplified by compound **7** and by the previously reported compound $(Cs_{0.75}K_{0.25})U_2(Nb,Ti)O_{11}$ [65].

6. Conclusion

Depending on the nature of the alkaline metal, layered or tunneled uranyl niobates are prepared. Layered compounds $AUNbO_6$ are obtained in this work for A = Li and Cs with layers of two types built from uranium pentagonal bipyramids and niobium square pyramids. For A = Li, the layers result from edge sharing of $^1_\infty[UO_5]^{4-}$ chains of edge-shared UO_7 polyhedra and $^1_\infty[NbO_4]^{3-}$ chains of corner-shared NbO_5 polyhedra. Compounds with

Table 10
Crystallographic characteristics of the up-to-day reported vanadates and niobates of uranyl and alkaline metal with formula $A_{1-x}UMO_{6-x/2}$ for $x = 0$ and 0.5

	a (Å)	b (Å)	c (Å)	β (deg)	Structure-type	Ref.
$NaUVO_6$	5.993(2)	8.344(2)	10.417(2)	100.38(3)	Carnotite layer	[40–43]
$KUVO6$	6.599(1)	8.403(2)	10.465(2)	104.01(2)	Carnotite layer	[40–43]
$RbUVO6$	6.904(1)	8.406(1)	10.472(2)	105.45(1)	Carnotite layer	[40–43]
$CsUVO6$	7.307(1)	8.449(1)	10.525(2)	106.04(1)	Carnotite layer	[40–43]
$LiUNbO6 \cdot 2H2O$	8.88(2)	11.52(1)	13.65(2)		$KUNbO6$ type layer	[56]
$LiUNbO6$	8.73(1)	13.22(1)	10.04(1)		$KUNbO6$ type layer	[56]
	10.309(1)	6.441(1)	7.5602(5)	100.65(1)	New layer structure	This work
$NaUNbO_6 \cdot H_2O$	9.04(4)	11.57(2)	12.17(2)		$KUNbO_6$ type layer	[62]
$NaUNbO_6$	8.71(2)	13.37(1)	10.28(1)		$KUNbO_6$ type layer	[62]
	13.3777(5)	7.0010(2)	7.9282(2)	117.25(1)	Unknown structure	This work
$KUNbO_6$	7.579(2)	11.321(4)	15.249(5)		$KUNbO_6$ type layer	[44]
	10.307(2)	7.588(1)	13.403(2)		Tunneled structure	This work
$RbUNbO_6$	7.627(2)	11.420(4)	15.739(5)		$KUNbO_6$ type layer	[44]
	6.94(9)	8.40(0)	10.50(5)	105.4	Carnotite layer	[63]
$Rb_{0.5}UNbO_{5.75}$	10.432(3)	7.681(2)	13.853(4)		Tunneled structure	This work
$CsUNbO_6$	7.430(1)	8.700(1)	10.668(2)	105.08(1)	Carnotite layer	[45]
	7.4448(1)	8.7199(2)	10.6901(2)	105.064(1)	Carnotite layer	This work
$Cs_{0.5}UnbO_{5.75}$	10.607(2)	7.748(2)	13.952(3)		Tunneled structure	This work

similar layers have been previously described for $A = K$ and Rb [44]; we were unable to synthesize these compounds. For $A = Cs$, the layers are similar to those of the carnotite-type compounds $AUVO_6$ [45]. For $A = K$, the structure of the $KUNbO_6$ compound prepared in this work is built on a three-dimensional framework that results from edge sharing of $^1_\infty[UO_5]^{4-}$ chains and $^1_\infty[Nb_2O_8]^{6-}$ ribbons, two octahedral wide, creating large elliptic tunnels running down the [010] and occupied by K^+ ions. Similar frameworks are obtained in the homeotypic compounds $A_{0.5}UNbO_{5.75}$ for $A = Rb$ and Cs. For $A = Rb$, the cationic site within the tunnels is half-occupied as in the previously reported compound $Tl_{0.5}UNbO_{5.75}$ [44]. For $A = Cs$, the polyhedral framework which is built around the large alkaline metal is more symmetric and the tunnel section is a square. In these $A_{0.5}UNbO_{5.75}$ compounds, the cation deficit is compensated by partial oxygen site vacancy.

The reasons for which Gasperin obtained layered compounds $AUNbO6$ for $A = K$ and Rb are not obvious. Using the synthesis conditions of Gasperin, we obtained single crystals having the tunneled structure reported in the paper. The powder corresponding to the Gasperin compounds cannot be obtained. On the other hand, we are able to synthesize our compounds in quantity. At most, one can say that (1) the formation of the tunneled structure requires the presence of a large cation which plays a template role, (2) the layered structure is perhaps stabilized by substitution of Nb by, for example, V which supports layered structures. Further studies are needed, in particular ion exchanges and substitutions, both on the alkaline and the niobium sites, to determine the role of doping agents in the stabilization of layered or tunneled structures which would be of interest for the immobilization of ^{137}Cs. The possibility of "pumping" Cs by uranium–niobium oxides, as already shown by Gasperin [65], is also of interest for decontamination. Measurements of conductivity properties are also planned, as a matter of fact, layered and tunneled characters of the structures are favorable to cationic mobility; moreover, the introduction of oxygen vacancies could generate oxygen mobility.

References

[1] P.C. Burns, R.A. Olson, R.J. Finch, J.M. Hanchar, Y. Thibault, J. Nucl. Mater. 278 (2000) 290.
[2] J.M. Jackson, P.C. Burns, Can. Mineral. 39 (1) (2001) 187.
[3] Y. Li, P.C. Burns, J. Nucl. Mater. 299 (2001) 219.
[4] J.A. Danis, W.H. Runde, B. Scott, J. Fettinger, B. Eichhorn, Chem. Commun. 22 (2001) 2378.
[5] A.J. Locock, P.C. Burns, J. Solid State Chem. 163 (2002) 275.
[6] A.J. Locock, P.C. Burns, J. Solid State Chem. 167 (2002) 226.
[7] S.V. Krivovichev, P.C. Burns, Can. Mineral. 39 (1) (2001) 207.
[8] I. Duribreux, Thesis, UST-Lille, 1997.
[9] S.V. Krivovichev, C.L. Cahill, P.C. Burns, Inorg. Chem. 42 (7) (2003) 2459.
[10] S.V. Krivovichev, C.L. Cahill, P.C. Burns, Inorg. Chem. 41 (1) (2001) 34.
[11] S.V. Krivovichev, R.J. Finch, P.C. Burns, Can. Mineral. 40 (1) (2002) 193.
[12] S.V. Krivovichev, P.C. Burns, Can. Mineral. 39 (1) (2001) 197.
[13] S.V. Krivovichev, P.C. Burns, Can. Mineral. 40 (1) (2002) 201.
[14] S. Obbade, C. Dion, M. Saadi, S. Yagoubi, F. Abraham, J. Solid State Chem. 174 (2003) 19.
[15] S.V. Krivovichev, P.C. Burns, Can. Mineral. 38 (2000) 717.
[16] S. Yagoubi, Thesis, UST-Lille, 2004.
[17] S. Obbade, C. Dion, E. Bekaert, S. Yagoubi, M. Saadi, F. Abraham, J. Solid State Chem. 172 (2003) 305.
[18] S.V. Krivovichev, P.C. Burns, Solid State Sci. 5 (2003) 373.
[19] S. Obbade, S. Yagoubi, C. Dion, M. Saadi, F. Abraham, J. Solid State Chem. 177 (2004) 1681.
[20] R.E. Sykora, T.E. Albrecht-Schmitt, J. Solid State Chem. 177 (2004) 3729.
[21] I. Duribreux, C. Dion, M. Saadi, F. Abraham, J. Solid State Chem. 146 (1999) 258.
[22] C. Dion, S. Obbade, E. Raekelboom, M. Saadi, F. Abraham, J. Solid State Chem. 155 (2000) 342.
[23] M. Saadi, C. Dion, F. Abraham, J. Solid State Chem. 150 (2000) 72.
[24] S. Obbade, C. Dion, L. Duvieubourg, M. Saadi, F. Abraham, J. Solid State Chem. 173 (2003) 1.
[25] I. Duribreux, M. Saadi, S. Obbade, C. Dion, F. Abraham, J. Solid State Chem. 172 (2003) 351.
[26] S. Obbade, C. Dion, M. Saadi, F. Abraham, J. Solid State Chem. 177 (2004) 1567.
[27] S. Obbade, C. Dion, M. Rivenet, M. Saadi, F. Abraham, J. Solid State Chem. 177 (2004) 2058.
[28] S. Obbade, C. Dion, M. Saadi, S. Yagoubi, F. Abraham, J. Solid State Chem. 177 (2004) 3909.
[29] L.M. Kovba, Radiokhimiya 13 (1971) 909.
[30] R. Chevalier, M. Gasperin, Bull. Soc. Fr. Mineral. Cristallogr. 93 (1970) 18.
[31] P.G. Dickens, C.P. Stuttard, R.G.J. Ball, A.V. Powell, S. Hull, S. Patat, J. Mater. Chem. 2 (2) (1992) 161.
[32] A.M. Chippindale, S.J. Crennell, P.G. Dickens, J. Mater. Chem. 5 (1993) 33.
[33] M. Schleifer, J. Busch, R. Gruehn, Z. Anorg. Allg. Chm. 625 (1999) 1985.
[34] R. Chevalier, M. Gasperin, C.R. Acad. Sci. Paris 267 (1968) 481.
[35] P.G. Dickens, G.J. Flynn, S. Patat, G.P. Stuttard, J. Mater. Chem. 7 (1997) 537.
[36] M. Labeau, I.E. Grey, J.C. Joubert, J. Chenavas, A. Collomb, J.C. Guitel, Acta Crystallogr. B 41 (1985) 33.
[37] R. Chevalier, M. Gasperin, Acta Crystallogr. B 28 (1972) 985.
[38] M.-C. Saine, J. Less-Common Met. 139 (1988) 315.
[39] F. Abraham, C. Dion, M. Saadi, J. Mater. Chem. 3 (5) (1993) 459.
[40] F. Abraham, C. Dion, N. Tancret, M. Saadi, Adv. Mater. Res. 1-2 (1994) 511.
[41] M. Saadi, Thesis, Lille, 2001.
[42] P.B. Barton, J. Am. Miner. 43 (1958) 799.
[43] D.E. Appleman, H.T. Evans, J. Am. Miner. 50 (1965) 825.
[44] M. Gasperin, J. Solid State Chem. 67 (1987) 219.
[45] M. Gasperin, Acta Crystallogr. C 43 (1987) 404.
[46] G.M. Sheldrick, SAINT Plus version 5.00, Bruker Analytical X-ray Systems, Madison, WI, 1998.
[47] G.M. Sheldrick, SHELXTL NT, Program Suite for solution and Refinement of Crystal Structure, version 5.1, Bruker Analytical X-ray Systems, Madison, WI, 1998.
[48] G.M. Sheldrick, Acta Crystallogr. A 51 (1995) 33.
[49] J. Rodriguez-Carvajal, M.T. Fernandez-Diaz, J.L. Martinez, J. Phys.: Condens. Mater. 3 (1991) 3215.
[50] P.E. Werner, L. Erikson, M. Westdhal, J. Appl. Crystallogr. 18 (1985) 367.
[51] D. Louer, M. Louer, J. Appl. Crystallogr. 5 (1972) 271.
[52] A. Boultif, D. Louer, J. Appl. Crystallogr. 24 (1991) 987.
[53] P.C. Burns, R.C. Ewing, F.C. Hawthorne, Can. Mineral. 35 (1997) 1551.

[54] N.E. Brese, M. O'Keeffe, Acta Crystallogr. B 47 (1991) 192.
[55] P.G. Dickens, G.P. Stuttard, J. Mater. Chem. 2 (1992) 691.
[56] T.L. Cremers, P.G. Eller, R.A. Penneman, C.C. Heerick, Acta Crystallogr. 39 (1983) 1163.
[57] P. Benard, D. Loüer, N. Dacheux, V. Brandel, M. Genet, Chem. Mater. 6 (1994) 1049.
[58] N. Tancret, S. Obbade, F. Abraham, Eur. J. Solid. State Inorg. Chem. 32 (1995) 195.
[59] A.M. Chippindale, P.G. Dickens, G.J. Flynnand, C.P. Stuttard, J. Mater. Chem. 5 (1995) 141.
[60] P.C. Burns, M.L. Miller, R.C. Ewing, Can. Mineral. 34 (1996) 845.
[61] P.C. Burns, Can. Mineral. 43 (2005) 1839.
[62] O.G. D'yachenko, V.V. Tabachenko, R. Tali, L. Kovba, B.O. Marinder, M. Sundberg, Acta Crystallogr. B 52 (1996) 961.
[63] N.G. Chernorukov, E.V. Suleimonov, N.P. Egorov, I.M. Romanenko, Russ. J. Gen. Chem. 64 (1994) 1.
[64] N.G. Chernorukov, N.P. Egorov, E.V. Suleimonov, Radiokhimiya 34 (1992) 17.
[65] M. Gasperin, Acta Crystallogr. C 42 (1986) 136.